

# Dietary Energy Intake and Presence of Aberrant Crypt Foci Are Associated with Phospholipid, Purine, and Taurine Metabolite Abundances in C57BL/6N Mouse Colon

Haley A. Chatelaine, Cynthia A. Ramazani, Kyle Spencer, Susan Olivo-Marston, Michael T. Bailey, Joseph McElroy, Emmanuel Hatzakis, Ewy A. Mathé,\* and Rachel E. Kopec\*

**Scope:** Colon metabolomes associated with high-fat (H) versus energy-restricted (E) diets in early colorectal cancer (CRC) models have never been directly compared. The objectives of this study are to elucidate metabolites associated with diet, aberrant crypt foci (ACF), and diet:ACF interaction, using a lifetime murine model.

**Methods and results:** Three-week-old mice consumed control (C), E, or H initiation diets for 18 weeks. ACF formation is initiated weeks 16–21 with azoxymethane injections, followed by progression diet crossover (to C, E, or H) through week 60. Colon extracts are analyzed using ultra-high-performance liquid chromatography-high resolution mass spectrometry (UHPLC-HRMS). Metabolites associated with diet, ACF, or diet:ACF are determined using regression models (FDR-adjusted  $p$ -value <0.05). No metabolites are significantly associated with initiation diets, but concentrations of acylcarnitines and phospholipids are associated with C, E, and H progression diets. Purines, taurine, and phospholipids are associated with ACF presence. No significant associations between metabolites and diet:ACF interaction are observed.

**Conclusions:** These results suggest that recent, rather than early-life, diet is more closely associated with the colon metabolome, particularly lipid metabolism. Results from this study also provide candidate biomarkers of early CRC development and provide support for the importance of early diet on influencing pre-CRC risk.

## 1. Introduction

Colorectal cancer (CRC) has the second highest mortality rate among cancers worldwide.<sup>[1]</sup> However, localized colorectal tumors, if identified early in development, have one of the highest survival rates of all cancer types.<sup>[2]</sup> Although a variety of screening procedures for CRC exist, they are not implemented uniformly due to low sensitivity or to high invasiveness/cost.<sup>[3]</sup> Identifying early markers reflective of underlying biological changes that drive CRC is necessary to decrease burden. Aberrant crypt foci (ACF) are the earliest potential precursor for CRC development and arise due to changes in colon epithelial cell division and proliferation.<sup>[4]</sup> Metabolites that signify and/or facilitate the changes associated with ACF formation may shed light on their origins and serve as early biomarkers of future CRC development.

Because the majority of CRC cases arise sporadically,<sup>[5]</sup> modifiable risk factors like diet have been implicated in up to 70% of CRC risk.<sup>[6]</sup> Epidemiological studies reveal a high positive correlation


H. A. Chatelaine, R. E. Kopec  
 OSU Interdisciplinary Nutrition PhD Program (OSUN)  
 Department of Human Sciences  
 The Ohio State University  
 1787 Neil Ave, Columbus, OH 43210, United States  
 E-mail: kopec.4@osu.edu

H. A. Chatelaine, K. Spencer, E. A. Mathé  
 Division of Preclinical Innovation Informatics Core  
 National Center for Advancing Translational Sciences  
 9800 Medical Center Drive, Rockville, MD 20850, USA  
 E-mail: ewy.mathe@nih.gov

C. A. Ramazani, K. Spencer, J. McElroy, E. A. Mathé  
 Department of Biomedical Informatics  
 The Ohio State University  
 Columbus, OH 43210, USA

C. A. Ramazani  
 Big Data for Indiana State University  
 Indiana State University  
 Terre Haute, IN 47807, USA

K. Spencer, M. T. Bailey  
 Nationwide Children's Hospital  
 Columbus, OH 43205, USA

 The ORCID identification number(s) for the author(s) of this article can be found under <https://doi.org/10.1002/mnfr.202200180>

© 2022 The Authors. Molecular Nutrition & Food Research published by Wiley-VCH GmbH. This is an open access article under the terms of the Creative Commons Attribution-NonCommercial-NoDerivs License, which permits use and distribution in any medium, provided the original work is properly cited, the use is non-commercial and no modifications or adaptations are made.

DOI: 10.1002/mnfr.202200180

between a high-fat (H) diet and risk of CRC development.<sup>[7–9]</sup> These findings have been corroborated in murine studies in which H diets led to increased tumor weight,<sup>[10]</sup> ACF formation,<sup>[11]</sup> and polyp size,<sup>[12]</sup> as compared to controls fed normocaloric diets. In contrast, murine models of calorie restriction suggest that fewer and smaller tumors or polyps develop in those receiving energy-restricted (E) diets, regardless of the method of cancer initiation.<sup>[13–15]</sup> Observational studies in Nordic countries ( $n = 256,073$ ) and the Netherlands Cohort study ( $n = 120,852$ ) also reported trends toward lower incidence of CRC among cohorts who experienced famine during World War II as compared to cohorts who did not, providing further evidence that calorie restriction may be associated with decreased CRC risk in humans.<sup>[16,17]</sup>

Metabolomics techniques, generally liquid chromatography-high resolution mass spectrometry (LC-HRMS) or nuclear magnetic resonance spectroscopy (NMR), can aid in identifying candidate diet biomarkers that concomitantly associate with early CRC development. These putative biomarkers can be further investigated in targeted experiments to validate associations with CRC development, as well as identify potential pathways that may reflect early opportunities for therapeutic intervention.

While the influence of high-fat (H)<sup>[18]</sup> and energy-restricted (E)<sup>[19]</sup> diets on the colon metabolome have been investigated independently, they have not been directly compared within the same experiment. Thus, the objective of this study was to compare colon metabolites following the consumption of H, E, or

control (C) diets, as well as their association with ACF formation. Samples from a previously published study by Xu et al.<sup>[20]</sup> were leveraged. In the original study, the initiation diet was shown to influence the number of ACF detected in each murine colon, while the progression diet had a less pronounced influence on ACF.<sup>[20]</sup> Surprisingly, E progression diet was associated with increased numbers of ACF, contrary to expectations based on previous studies noted above.<sup>[16,17]</sup> Based upon previous fecal results,<sup>[21]</sup> we hypothesized that later life (i.e., progression) diet would be more reflective of the current colon metabolome relative to earlier life (i.e., initiation) diets. We anticipated that metabolite classes previously identified in H versus C diets (e.g., decreased bile acids and increased unsaturated fatty acids),<sup>[18]</sup> and E versus C diets (e.g., increased vitamin E metabolites and decreased amino acids<sup>[19]</sup>) would be associated with diet, and hypothesized more dramatic fold changes in comparing H versus E. We also hypothesized that we would observe metabolites unique to ACF presence/absence, and a diet:ACF interaction significantly associated with metabolite concentrations. We tested these hypotheses using regression models of metabolomics profiles for the following three questions: 1) are any metabolites associated with initiation or progression diet? 2) Are any metabolites associated with ACF presence? 3) Are any metabolites associated with an interaction between diet (initiation or progression) and ACF presence?

## 2. Experimental Section

### 2.1. Mouse Intervention and Colon Sample Collection

Mouse husbandry and dietary intervention were previously published.<sup>[20]</sup> This study was a secondary analysis of murine tissues collected from a previous protocol approved by the Institutional Animal Care and Use Committee (IACUC) at The Ohio State University (protocol #2011A00000074). Briefly, female C57BL/6N mice (Charles River, Wilmington, MA, USA) were fed a control (C), high fat (H), or energy restricted (E) diet from 3 to 21 weeks of age, hereafter referred to as the “initiation diet.” Diets were semi-purified (Research Diets, Inc., New Brunswick, NJ, USA) where C contained 10% kcal from fat (D12450B), H contained 45% kcal from fat (D12451), and E had 30% fewer kcals provided than C (D03020702) (full composition in Table S1, Supporting Information). Azoxymethane (AOM, Santa Cruz Biotechnology, Inc. Dallas, TX, USA) was administered as an intraperitoneal dose ( $10 \text{ mg kg}^{-1}$ ) weekly from weeks 16 to 21 of age. Mice were then either maintained or reassigned diets from weeks 22 to 60 of age (hereafter referred to as the “progression diet”) for a  $3 \times 3$  design (CC  $n = 33$ , CH  $n = 35$ , CE  $n = 34$ , HC  $n = 24$ , HH  $n = 24$ , HE  $n = 24$ , EC  $n = 30$ , EH  $n = 24$ , EE  $n = 38$ ). Mice were sacrificed at 60 weeks, and the proximal, medial, and distal colon were removed (Figure S1, Supporting Information). Samples were stored at  $-80^\circ\text{C}$ .

### 2.2. Monophasic Sample Extraction

Colon samples (2–10 mg) were thawed in cold water and weighed (XS105 DualRange, Mettler Toledo, Columbus, OH, USA) (2–10 mg). Ice-cold solvent, 2:5:2  $\text{CDCl}_3/\text{CD}_3\text{OH}/\text{H}_2\text{O}$  (v/v/v), was

---

S. Olivo-Marston  
Division of Epidemiology  
College of Public Health  
The Ohio State University  
Columbus, OH 43210, USA

S. Olivo-Marston  
Southern Illinois University School of Medicine  
Springfield, IL 62794, USA

M. T. Bailey  
Department of Pediatrics  
The Ohio State University College of Medicine  
Columbus, OH 43210, USA

M. T. Bailey  
Center for Microbial Pathogenesis  
Nationwide Children's Hospital  
Columbus, OH 43205, USA

M. T. Bailey  
Oral and GI Research Affinity Group  
Nationwide Children's Hospital  
Columbus, OH 43205, USA

E. Hatzakis  
Department of Food Science and Technology  
The Ohio State University  
Columbus, OH 43210, USA

E. Hatzakis, R. E. Kopec  
Foods for Health Discovery Theme  
The Ohio State University  
Columbus, OH 43210, USA

E. A. Mathé  
Comprehensive Cancer Center  
The Ohio State University  
Columbus, OH 43210, USA

E. A. Mathé  
Translational Data Analytics Institute  
The Ohio State University  
Columbus, OH 43210, USA

added (850  $\mu\text{L}$ ) with zirconia beads (0.05 mm, BioSpec Products, Bartlesville, OK, USA). Deuterated solvents were used to enable LC-MS and NMR analysis. Samples were ground (Minibeater-16, BioSpec Products, Bartlesville, OK, USA) for 3 min, cooled on ice for 5 min, repeated for three cycles. Ground samples were centrifuged for 2 min at  $12\,000 \times g$  at  $4^\circ\text{C}$  (Microfuge 22R, Beckman Coulter, Brea, CA, USA), the supernatant (750  $\mu\text{L}$ ) was centrifuged a second time to remove particulate. Extracts were stored at  $-80^\circ\text{C}$ .

### 2.3. HILIC UHPLC-MS Analysis

Extracts were thawed and centrifuged for 5 min at  $12\,000 \times g$  and  $4^\circ\text{C}$  and analyzed using a method adapted from Gowda et al.<sup>[22]</sup> Extracts were injected (10  $\mu\text{L}$ ) into an Agilent 1290 UHPLC with an Agilent Poroshell 120 HILIC-Z column (2.1  $\times$  100 mm, 1.9  $\mu\text{m}$  particle size) at  $35^\circ\text{C}$ . Solvent A = 95:5 water/acetonitrile (v/v) with 0.2% aq. acetic acid and 5 mM ammonium acetate, and solvent B = 95:5 acetonitrile/water (v/v) with 0.2% aq. acetic acid (positive mode only) and 5 mM ammonium acetate. A flow rate of 0.3  $\text{mL min}^{-1}$  was used with a gradient beginning with 99% solvent B held for 1 min, decreased to 40% B over 9 min, and returned to 99% B over 6 min.

The UHPLC was interfaced with an Agilent 6545 quadrupole time-of-flight mass spectrometer (QToF-MS) with a Dual Agilent Jet Stream electrospray ionization (ESI) probe operated in positive and negative modes. Source parameters: drying gas temperature =  $300^\circ\text{C}$ , drying gas flow = 10  $\text{L min}^{-1}$ , sheath gas temperature =  $350^\circ\text{C}$ , sheath gas flow = 12  $\text{L min}^{-1}$ , nebulizer pressure = 25 psig, voltage capillary = 3000 V, fragmentor = 100 V, skimmer = 45 V, optical lens = 750 V. The instrument was operated in full scan mode over 50–1700  $m/z$ , collecting 8119 transients per spectrum (1 spectrum  $\text{s}^{-1}$ ). Process blanks were analyzed every 15th injection. Pooled QCs were analyzed every 10th injection. One representative sample from each diet group was also analyzed using iterative MS/MS fragmentation for metabolite identification.

### 2.4. NMR Analysis

Insufficient signal intensity relative to impurities also extracted in process blanks, due to low sample weight, precluded differentiation of  $^1\text{H-NMR}$  spectra from process blanks. Only UHPLC-MS data were used for further analysis (data collection details in supplement).

### 2.5. UHPLC-MS Metabolomics Data Pre-Processing

#### 2.5.1. Data Deconvolution and Feature Extraction

Raw UHPLC-MS data from the pooled QC samples and process blanks were deconvoluted, aligned, and grouped using Agilent Profinder (B.08 SP3, Agilent, Santa Clara, CA, USA) recursive batch feature extraction, with a retention time window from 1.5 to 13.5 min, noise cutoff of 3000 ion counts, retention time tolerance of 0.2 min, and mass tolerance of 20 ppm. The resulting

metabolites were manually inspected to remove compounds that were present in process blanks, correct errors in integration, and eliminate incorrectly extracted non-peaks. The resulting metabolite list was then used for a targeted feature extraction of the samples and re-extraction of the pooled QCs. Further manual inspection of peak quality, following the same guidelines, yielded 491 and 415 total metabolites in positive and negative modes, respectively.

#### 2.5.2. Data Preparation for Linear Regression Analyses

The data preparation workflow was given in Figure S2, Supporting Information and described in the supplementary methods. Metabolites with a coefficient of variation  $>30\%$  in the pooled QC samples were removed, yielding 365 and 414 metabolites in positive and negative modes, respectively. Of these metabolites, 122 duplicate peaks, which were erroneously extracted during the metabolite grouping, were removed (Supplementary methods, Figure S3, Supporting Information). Peaks with a standard deviation lower than the 5th percentile in each diet pair analyzed were removed. Ultimately, 624 metabolites remained as input in the linear regression models.

Unsupervised clustering of the samples was performed to evaluate the efficacy of batch correction and the possible influence of experimental factors such as batch number and sample weight (Figure S4–S6, Supporting Information).

#### 2.5.3. Aberrant Crypt Foci (ACF) Characterization

ACF count data for each colonic region was previously reported.<sup>[20]</sup> Due to an uneven distribution of ACF counts (Figure S7, Supporting Information), ACF were summed within an animal, across all colon regions, and were characterized in binary form: 0 ACF as “absent” ( $n = 137$ ), at least 1 ACF as “present” ( $n = 129$ ).

#### 2.5.4. Regression Modeling

The proportion of ACF presence/absence was compared across diet groups using a logistic regression model, constructed using the `glm()` function (family set to binomial) of the ISLR package in R version 1.2,<sup>[23]</sup> that controlled for colon region and mouse cohort from the original study:

$$\text{ACF Presence} \sim \text{Diet Group} + \text{Cohort} + \text{Colon Region} \quad (1)$$

Pairwise linear mixed-effects regression models (18 diet pairs) were performed to evaluate the effects of diet, ACF, and diet:ACF on metabolite levels. The initiation or the progression diet was held constant within each diet pair compared (Equation (2), Table S2, Supporting Information). Three measurements were made per mouse (proximal, medial, and distal sections), so mouse ID numbers were used as random effects. The mixed-effect models were constructed using the R `nlme` package version 3.1-152.<sup>[24]</sup>

$$\begin{aligned} \text{Metabolite Intensity} \sim & \text{Diet Group} + \text{ACF Presence} \\ & + \text{Tissue Weight} + 1 \mid \text{Mouse ID} \end{aligned} \quad (2)$$

Metabolites with an FDR-adjusted  $p$ -value  $\leq 0.05$  were considered for diet and ACF associations.

A linear mixed-effect model on the same 18 diet pairs (Equation (3)) was used to determine an interaction between diet groups and ACF presence.

$$\text{Metabolite} \sim \text{Diet Group} + \text{ACF} + \text{Diet Group} : \text{ACF} \\ + \text{Tissue Weight} + 1 \mid \text{Mouse ID} \quad (3)$$

## 2.6. Identification of Metabolite Groups

Metabolites were selected for identification if they a) had a false discovery rate (FDR) adjusted  $p$ -value  $\leq 0.05$  and b) were in the top 20 highest absolute value of linear model estimate in at least one diet comparison for diet, or top 20 highest and lowest values for ACF in Equation (2). Identification methodology was described in Supplemental Methods, and confidence levels were assigned following established standards.<sup>[25]</sup> Despite computational removal of duplicate peaks, some metabolites retained for identification were redundant, leaving 98 significant metabolites for identification in the diet comparison and 31 metabolites in the ACF comparison. Unidentified but significant metabolites were listed in Table S3, Supporting Information for diet comparisons and Table S4, Supporting Information for ACF comparisons.

## 2.7. Pathway Analysis

Identified metabolites with HMDB<sup>[26]</sup> or LIPIDMAPS<sup>[27]</sup> identifiers were input into the web interface of the Relational Metabolomic Pathway Database (RaMP),<sup>[28]</sup> using a generic background. Enriched pathways with FDR-adjusted  $p$ -values less than 0.2 were used to determine pathways of interest for hypothesis generation. Additional pathways that were not reported by RaMP analyses were hypothesized based on literature precedence for identified metabolites.

## 2.8. Data Availability

Data are available at Figshare.com in the private DOIs listed in Table 1.

## 3. Results

HILIC UHPLC-MS metabolite profiles were compared between mice consuming H, E, or C diets in the initiation and/or progression phase of ACF presence. Regression modeling of metabolites associated with diet or ACF (Equation (2)) yielded significantly different metabolites due to progression diet and presence/absence of ACF.

### 3.1. Metabolites Associated with Diet

To answer the first question (metabolite associations with diet), nine regression models with different *initiation* diets were compared, holding the progression diet constant (CC vs EC, CC vs

**Table 1.** Private DOI links to study data.

Data description	DOI
HILIC positive mode QC and blank raw data	<a href="https://figshare.com/s/6da67608118757ce8df4">https://figshare.com/s/6da67608118757ce8df4</a>
HILIC positive mode sample raw data	<a href="https://figshare.com/s/e7d0e37c7aac40c041b8">https://figshare.com/s/e7d0e37c7aac40c041b8</a>
HILIC negative mode all raw data (QC, blanks, samples)	<a href="https://figshare.com/s/b9f23ba2b80a03937a8a">https://figshare.com/s/b9f23ba2b80a03937a8a</a>
HILIC positive and negative grouped metabolite abundances	<a href="https://figshare.com/s/48913ea625223ecae306">https://figshare.com/s/48913ea625223ecae306</a>
HILIC positive and negative transformed and filtered metabolite abundances	<a href="https://figshare.com/s/3662f41987724c479333">https://figshare.com/s/3662f41987724c479333</a>
Sample meta-data	<a href="https://figshare.com/s/5a66d6367a4874f160cc">https://figshare.com/s/5a66d6367a4874f160cc</a>

HC, HC vs EC; CE vs EE, CE vs HE, HE vs EE; and CH vs EH, CH vs HH, HH vs EH). In eight models, no significant metabolites were found. The EE versus CE comparison was run without ACF as a covariate due to a previous convergence error. Even without this covariate, no significantly different metabolites were observed (Figure S8, Supporting Information).

The remaining nine regression models focused on *progression* diet comparison, holding initiation diet fixed (CC vs CE, CC vs CH, CH vs CE; EC vs EE, EC vs EH, EH vs EE; and HC vs HE, HC vs HH, HH vs HE). Significantly different metabolites for each are given in Table 2, and largely belong to acylcarnitine and phospholipid classes (Figures 1 and 2). Metabolite identities are provided in Table 2. Phosphatidylcholine catabolism and phospholipid biosynthesis pathways were enriched for metabolites of interest in diet comparisons (Table 3).

The proportion of ACF presence/absence was also considered between all diet pairs (data not shown). Only one diet pair, CC versus EH, had a significant difference in proportion of ACF presence, independent of study cohort or colon region (Equation (1)). Because this pair was not considered in our interpretation of diet results, all presented diet pairs reflect no differences in proportion of ACF presence.

### 3.2. Metabolites Associated with ACF

A total of 31 metabolites met  $p$ -value and fold-change cutoffs and were retained for identification for associations with ACF in the linear model (Figure 3, Table 4) to answer the second question. Mice that developed ACF had increased concentrations of multiple lyso-phosphatidylcholines (LPC), phosphatidylethanolamines (PE), phosphatidylcholines (PC), and one species, each, of a lyso-phosphatidylethanolamine (LPE), ether phosphatidylcholine (PC-O), and phosphatidylinositol (PI). In contrast, one cyclophosphatidic acid (CPA) and one ether phosphatidylethanolamine (PE-O) were reduced in mice with ACF. The intensity of purines and the amino acid taurine were also reduced in mice with ACF, relative to animals without ACF, as

**Table 2.** Identities of metabolites that met fold-change and *p*-value cutoffs in diet comparisons (FDR-adjusted *p*-value ≤0.05 and top 20 absolute value estimate for diet term in Equation (2) in at least one diet pair, see Figure 1).

<i>m/z</i> <sup>a)</sup>	RT [min]	Precursor ion	Ionization mode	Class	ID	ID level
400.3445	3.29	[M+H] <sup>+</sup>	Pos	Acylcarnitine	CAR(16:0)	1
428.3757	3.23	[M+H] <sup>+</sup>	Pos	Acylcarnitine	CAR(18:0)	1
426.3602	3.24	[M+H] <sup>+</sup>	Pos	Acylcarnitine	CAR(18:1)	1
424.3447	3.26	[M+H] <sup>+</sup>	Pos	Acylcarnitine	CAR(18:2)	1
204.1223	4.82	[M+H] <sup>+</sup>	Pos	Acylcarnitine	acetylcarnitine	2
398.3286	3.30	[M+H] <sup>+</sup>	Pos	Acylcarnitine	CAR(16:1)	2
442.3548	3.70	[M+H] <sup>+</sup>	Pos	Acylcarnitine	CAR(18:1;O)	3
498.2891	3.21	[M+Cl] <sup>-</sup>	Neg	Acylcarnitine	CAR(20:4)-hydroxy	3
460.2831	3.93	[M+C <sub>2</sub> H <sub>3</sub> O <sub>2</sub> ] <sup>-</sup>	Neg	Acylcarnitine	CAR(14:1;O <sub>2</sub> )	3
456.4063	3.17	[M+H] <sup>+</sup>	Pos	Acylcarnitine	CAR(20:0)	3
448.3450	3.21	[M+H] <sup>+</sup>	Pos	Acylcarnitine	CAR(20:4)	3
124.0073	5.41	[M-H] <sup>-</sup>	Neg	Amino acid	taurine	1
265.1132	4.71	[M] <sup>+</sup>	Pos	B vitamin	thiamin	1
415.2234	2.56	[M-H] <sup>-</sup>	Neg	Cyclophosphatidic acid	CPA(18:2)	2
419.2549	2.31	[M-H] <sup>-</sup>	Neg	Cyclophosphatidic acid	CPA(18:0)	2
439.2251	2.43	[M-H-H <sub>2</sub> O] <sup>-</sup>	Neg	Lysophosphatidic acid	LPA(20:4)	2
524.3751	3.73	[M+H] <sup>+</sup>	Pos	Lysophosphatidylcholine	LPC(18:0)	1
522.3587	3.65	[M+H] <sup>+</sup>	Pos	Lysophosphatidylcholine	LPC(18:1)	1
452.3161	3.85	[M+H] <sup>+</sup>	Pos	Lysophosphatidylcholine	LPE(16:1)	2
494.3277	3.71	[M+H] <sup>+</sup>	Pos	Lysophosphatidylcholine	LPC(16:1)	2
520.3439	3.67	[M+H] <sup>+</sup>	Pos	Lysophosphatidylcholine	LPC(18:2)	2
565.4041	3.97	[M+NH <sub>4</sub> ] <sup>+</sup>	Pos	Lysophosphatidylcholine	LPC(20:2)	3
623.5056	3.57	[M+NH <sub>4</sub> ] <sup>+</sup>	Pos	Lysophosphatidylcholine	LPC(24:1)	3
1045.7201	3.70	[2M-H] <sup>+</sup>	Pos	Lysophosphatidylcholine	in-source homodimer, LPC(18:1)	3
1099.6885	3.79	[2M-H] <sup>-</sup>	Neg	Ether lysophosphatidylcholine	in-source homodimer, LPC(O-18:2)	3
480.3463	3.64	[M+H] <sup>+</sup>	Pos	Lysophosphatidylethanolamine	LPE(18:1)	1
436.2833	3.95	[M-H] <sup>-</sup>	Neg	Lysophosphatidylethanolamine plasmalogen	LPE(P-16:0)	2
480.3091	4.03	[M-H] <sup>-</sup>	Neg	Lysophosphatidylethanolamine	LPE(18:0)	2
478.2962	3.90	[M+H] <sup>+</sup>	Pos	Lysophosphatidylethanolamine	LPE(18:2)	2
531.2794	3.36	[M-H] <sup>-</sup>	Neg	Lysophosphatidylglycerol	LPG(20:4)	3
703.5431	3.23	[M-H] <sup>-</sup>	Neg	Phosphatidic acid	PA(36:0)	3
1520.1696	2.73	[2M+H] <sup>+</sup>	Pos	Phosphatidylcholine	PC(16:0/18:1)	1
731.6070	2.93	[M+NH <sub>4</sub> ] <sup>+</sup>	Pos	Ether phosphatidylcholine	PC(O-32:3)	2
700.5300	3.04	[M+H] <sup>+</sup>	Pos	Phosphatidylcholine	PC(30:3)	3
1503.0934	3.10	[M+M-2H] <sup>-</sup>	Neg	Phosphatidylcholine	in-source heterodimer, PC(16:0/18:1) + PC(O-16:0/18:1)	3
1527.1021	3.08	[M+M-2H] <sup>-</sup>	Neg	Phosphatidylcholine	in-source heterodimer, PC(16:0/20:4) + PC(O-16:0/18:0)	3
674.5143	3.08	[M+H-H <sub>2</sub> O] <sup>+</sup>	Pos	Phosphatidylethanolamine	PE(16:0/16:0)	1
716.5222	3.25	[M-H] <sup>-</sup>	Neg	Phosphatidylethanolamine	PE(16:0/18:1)	1
688.4968	3.28	[M-H] <sup>-</sup>	Neg	Phosphatidylethanolamine	PE(16:0/16:1)	2
832.6208	3.02	[M-H] <sup>-</sup>	Neg	Phosphatidylethanolamine	PE(43:6)	3
804.5887	3.04	[M-H] <sup>-</sup>	Neg	Phosphatidylethanolamine	PE(41:6) or PE(O-42:6)	3
778.5740	3.07	[M-H] <sup>-</sup>	Neg	Phosphatidylethanolamine	PE(39:5) or PE(O-40:5)	3
780.5853	3.10	[M-H] <sup>-</sup>	Neg	Phosphatidylethanolamine	PE(39:4) or PE(O-40:4)	3
756.5887	3.18	[M-H] <sup>-</sup>	Neg	Phosphatidylethanolamine	PE(37:2) or PE(O-38:2)	3
706.4839	3.24	[M-H] <sup>-</sup>	Neg	Phosphatidylethanolamine	PE(34:6)	3
714.5096	3.25	[M-H] <sup>-</sup>	Neg	Phosphatidylethanolamine	PE(34:2)	3

(Continued)

**Table 2.** (Continued).

$m/z^a$	RT [min]	Precursor ion	Ionization mode	Class	ID	ID level
1505.1090	3.10	[2M-2H] <sup>-</sup>	Neg	Ether phosphatidylethanolamine	in-source homodimer, PE(O-38:4)	3
747.5176	2.26	[M-H] <sup>-</sup>	Neg	Phosphatidylglycerol	PG(16:0/18:1)	2
884.5366	3.54	[M-H] <sup>-</sup>	Neg	Phosphatidylinositol	PI(20:4/18:1)	2
857.5185	3.58	[M+Cl] <sup>-</sup>	Neg	Ether phosphatidylinositol	PI(O-34:1)	3
931.6140	3.94	[M-H] <sup>-</sup>	Neg	Ether phosphatidylinositol	PI(O-42:2)	3
786.5281	3.85	[M-H] <sup>-</sup>	Neg	Phosphatidylserine	PS(36:2)	3
745.6245	3.45	[M+H] <sup>+</sup>	Pos	Sphingomyelin	SM(37:1;O2)	3
731.6119	3.46	[M+H] <sup>+</sup>	Pos	Sphingomyelin	SM(36:1;O2)	3
733.6184	3.46	[M+H] <sup>+</sup>	Pos	Sphingomyelin	SM(36:0;O2)	3
717.5945	3.47	[M+H] <sup>+</sup>	Pos	Sphingomyelin	SM(35:1;O2)	3

<sup>a</sup>) Unknown metabolites (level 4 ID) in Table S3, Supporting Information.

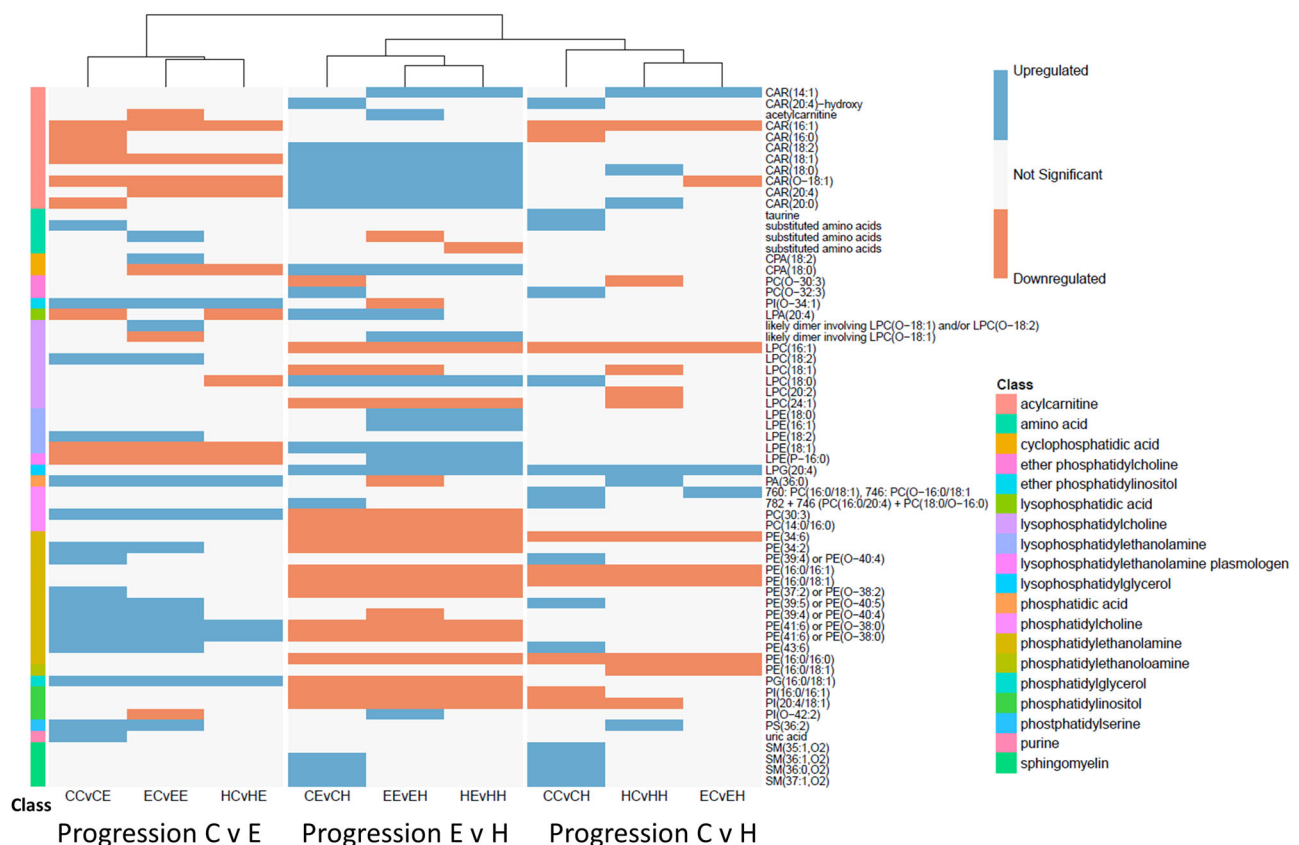


**Figure 1.** Heatmap of identified metabolites (FDR-adjusted  $p$  value <0.05; absolute value of estimate coefficient in top 20 in at least one comparison) in progression diet comparisons. Orange cell colors indicate metabolites that were significantly increased in the first progression diet group listed in the comparison, and blue cell colors indicate metabolites that were significantly increased in the second progression diet group listed. Metabolite classes are indicated by color in the left margin. C, control diet ( $n = 87$ ); E, energy-restricted diet ( $n = 96$ ); H, high-fat diet ( $n = 83$ ). The first letter indicates initiation diet, the second indicates progression diet.

confirmed with level 1 confidence. Pathway analysis in RaMP<sup>[28]</sup> revealed enrichment of pathways related to purine metabolism (Table 3).

No metabolites met  $p$ -value and fold-change cutoffs for the third question regarding a diet:ACF presence interaction in any of the 18 diet pair comparisons.

## 4. Discussion

### 4.1. Metabolites Associated with Diet

Diet-specific metabolome associations were only significant when the progression diet (reflecting recent dietary intake), not

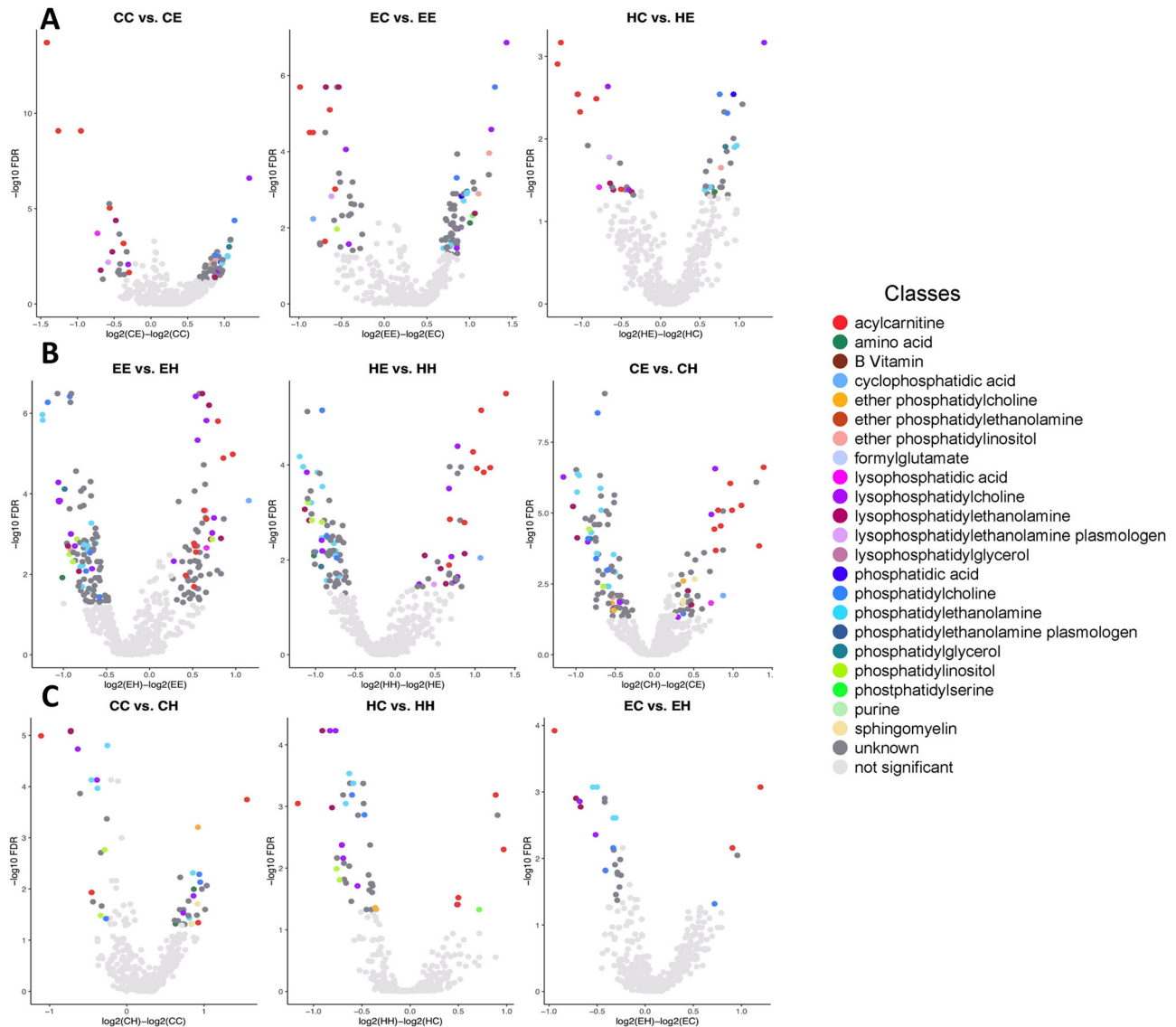


**Figure 2.** Volcano plots showing differences in  $\log_2$  fold-changes and  $p$ -values of metabolite classes in pairwise comparisons of the diet term in the linear model given in Equation (2), computed between mice that consumed different progression diets. A) Control (C) versus energy-restricted (E) (CC,  $n = 33$  vs CE,  $n = 34$ ; EC,  $n = 30$  vs EE,  $n = 38$ ; HC,  $n = 24$ , HE,  $n = 24$ ). B) Energy restricted (E) versus high-fat (H) (EE,  $n = 38$  vs EH,  $n = 24$ ; HE,  $n = 24$  vs HH,  $n = 24$ ; CE,  $n = 34$  vs CH,  $n = 35$ ). C) control (C) versus high-fat (H) (CC,  $n = 33$  vs CH,  $n = 35$ ; HC,  $n = 24$  vs HH,  $n = 24$ ; EC,  $n = 30$  vs EH,  $n = 24$ ). Significant metabolites met cutoffs of an FDR-adjusted  $p$ -value  $\leq 0.05$  and an absolute value of  $\log_2$ -fold change  $\geq 0.25$ . Metabolites with positive values were increased in the first diet listed relative to the second diet. Metabolites with negative values were decreased in the first diet listed, relative to the second diet.

the initiation diet, was different between groups. This finding is consistent with data suggesting human fecal metabolomic profiles better reflect more recent dietary consumption, compared to reported longer-term dietary intakes.<sup>[21]</sup>

Long-chain acylcarnitine species were consistently increased in progression H or C diet, compared with E diet. However, only some species of acylcarnitines were increased in progression H, compared to C diets. Similarly, H diets in rats were associated with increased serum concentrations of many long-chain acylcarnitine species, relative to controls.<sup>[29]</sup> Medium and long-chain acylcarnitines were also significantly

increased in the small, but not large, intestine, of piglets consuming the Western (i.e., high fat) versus Prudent diets.<sup>[30]</sup> A cross-sectional study of the Women's Health Initiative ( $n = 2199$ ) also noted that women who followed a Western diet had increased serum concentrations of medium and long-chain acylcarnitines, as compared with those following a Prudent diet pattern, even after controlling for known confounders (i.e., basal metabolic rate, energy intake).<sup>[31]</sup> Increased acylcarnitine concentrations in high-fat diets likely reflects increased flux through  $\beta$ -oxidation, where synthesis from cytosolic free fatty acids and carnitine serves as the rate limiting step.<sup>[32]</sup>

**Table 3.** Enriched pathways in RaMP,<sup>[2]</sup> following annotation of metabolites of interest for either diet or ACF associations (FDR *p*-value cutoff = 0.2).

Pathway	ID	Source	<i>p</i> -value	Number of metabolites enriched in pathway	Total metabolites in pathway	FDR <i>p</i> -value	Metabolites observed	Association for metabolites of interest
Purine metabolism	WP4792	Wiki	3.4E-06	4	37	<0.001	guanosine; hypoxanthine; inosine; uric acid	ACF
Purine metabolism and related disorders	WP4224	Wiki	2.4E-05	4	60	0.001	guanosine; hypoxanthine; inosine; uric acid	ACF
Purine catabolism	R-HSA-74259	Reactome	1.5E-04	4	61	0.003	guanosine; hypoxanthine; inosine; uric acid	ACF
Transport of nucleosides and free purine and pyrimidine bases across the plasma membrane	R-HSA-83936	Reactome	1.1E-04	3	21	0.003	guanosine; hypoxanthine; inosine	ACF
Nucleobase catabolism	WP4042	Wiki	1.9E-04	4	101	0.003	guanosine; hypoxanthine; inosine; uric acid	ACF
Nucleotide salvage	WP4082	Wiki	3.3E-04	3	46	0.004	guanosine; hypoxanthine; inosine	ACF
Purine salvage	R-HSA-74217	Reactome	4.1E-04	3	32	0.005	guanosine; hypoxanthine; inosine	ACF
Defective SLC29A3 causes histiocytosis-lymphadenopathy plus syndrome (HLAS)	R-HSA-5619063	Reactome	4.6E-04	2	7	0.005	guanosine; inosine	ACF
Nucleotide catabolism	R-HSA-8956319	Reactome	1.3E-03	4	107	0.008	guanosine; hypoxanthine; inosine; uric acid	ACF
Nucleotide salvage	R-HSA-8956321	Reactome	1.2E-03	3	46	0.008	guanosine; hypoxanthine; inosine	ACF
Nucleotide metabolism	WP404	Wiki	1.2E-03	2	17	0.008	hypoxanthine; uric acid	ACF
Transport of vitamins, nucleosides, and related molecules	WP1937	Wiki	1.0E-03	3	67	0.008	guanosine; hypoxanthine; inosine	ACF
Purine metabolism	map00230	Kegg	6.9E-03	4	68	0.030	guanosine; hypoxanthine; inosine; uric acid	ACF
Modified nucleosides derived from tRNA as urinary cancer markers	WP4485	Wiki	1.5E-03	2	19	0.009	guanosine; inosine	ACF
Phosphatidylcholine catabolism	WP4195	Wiki	1.7E-03	2	20	0.009	1-(11Z,14Z-eicosadienyl)-glycero-3-phosphocholine; 1-(5Z,8Z,11Z-eicosatrienyl)-sn-glycero-3-phosphocholine; 1-(15Z-tetracosaeenyl)-sn-glycero-3-phosphocholine; 1-(5Z,8Z,11Z,14Z-eicosatetraenyl)-sn-glycero-3-phosphate; Lyso-PA(20:4)	Diet
Phospholipid Biosynthesis	map00564	Kegg	2.8E-03	3	25	0.015	1,2-dihexadecanoyl-sn-glycero-3-phosphocholine; 1-(11Z,14Z-eicosadienyl)-glycero-3-phosphocholine; 1-(5Z,8Z,11Z-eicosatrienyl)-sn-glycero-3-phosphocholine; 1-(15Z-tetracosaeenyl)-sn-glycero-3-phosphocholine; 1,2-dihexadecanoyl-sn-glycero-3-phosphoethanolamine	Diet, ACF
Transport of vitamins, nucleosides, and related molecules	R-HSA-425397	Reactome	3.2E-03	3	64	0.016	guanosine; hypoxanthine; inosine	ACF
SLC transporter disorders	R-HSA-5619102	Reactome	6.2E-03	3	81	0.029	guanosine; inosine; uric acid	ACF
Disorders of transmembrane transporters	R-HSA-5619115	Reactome	1.1E-02	3	99	0.045	guanosine; inosine; uric acid	ACF
Transport of bile salts and organic acids, metal ions and amine compounds	WP1935	Wiki	2.0E-02	2	71	0.072	taurine; uric acid	ACF



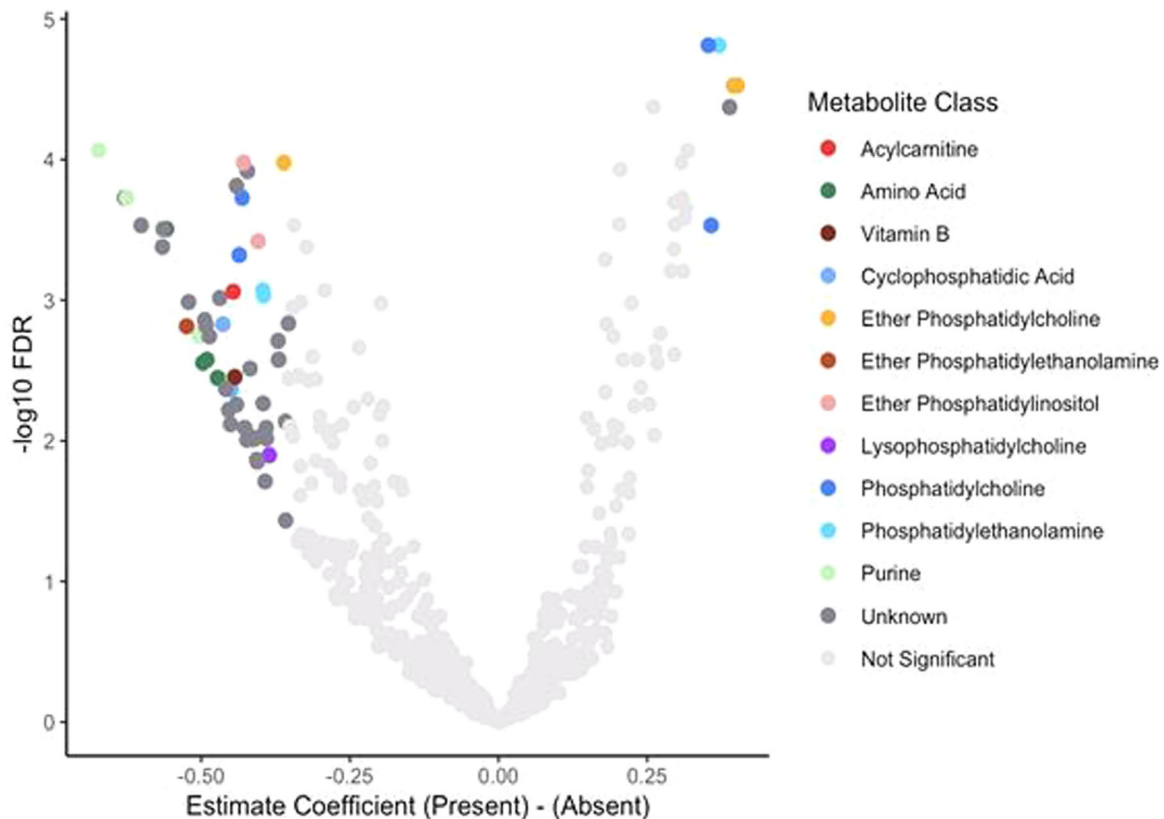


**Figure 3.** Volcano plots showing differences in  $\log_2$  fold-changes and  $p$ -values of metabolite classes in comparisons between samples with ACF present ( $n = 137$ ) versus absent ( $n = 129$ ), using the ACF term of the model given in Equation (2). Significant metabolites met cutoffs of an FDR-adjusted  $p$ -value  $\leq 0.05$  and an absolute value of  $\log_2$ -fold change  $\geq 0.335$  of the ACF term. Metabolite classes with positive values are increased in samples with ACF, and those with negative values are increased in samples without ACF.

Higher concentrations of acylcarnitines have been associated with various chronic diseases for which disorders of fatty acid oxidation are involved.<sup>[33]</sup>

Colon concentrations of PCs and PEs were higher, while saturated LPCs and LPEs were lower following E progression diet versus H or C progression diets. PEs were also increased in progression C versus progression H diets. Increases in PC and PE suggest less cleavage of fatty acids via phospholipase  $A_2$  (PLA<sub>2</sub>) to produce LPC and LPE, respectively, as suggested by the enrichment of PC catabolism in pathway analyses. PLA<sub>2</sub> is activated to produce eicosanoids during inflammation and is upregulated in the colonic mucosa of patients with ulcerative colitis, Crohn's disease,<sup>[34]</sup> and colorectal adenocarcinomas.<sup>[35]</sup> PC comprises  $\approx 90\%$  of the phospholipids of the colonic mucosa barrier, which protects the tissue against pathogenic microbial attack, which can incite/exacerbate these conditions.<sup>[36]</sup> Thus, higher PC concentrations are anticipated in tissue that remains intact. Additionally, all but one randomized, placebo-controlled trial providing slow-release PC to ulcerative colitis patients demonstrated dramatically increased rates of remission and improved clinical and endoscopic outcomes.<sup>[37]</sup> PE can serve as a precursor for PC through the phosphatidylethanolamine N-methyltransferase pathway.<sup>[38]</sup> PE induces cellular autophagy, which is upregulated under caloric restriction, and believed to be a primary target for reducing chronic disease risk.<sup>[39]</sup> Indeed, a normocaloric diet re-

sulted in lower concentrations of colon epithelium PEs in rats, relative to high fat diet.<sup>[40]</sup> Collectively, the evidence suggests that increased PC and PE concentrations, and lower saturated LPC and LPE concentrations, may reflect healthier colon cells and be associated with lower calorie diets.

Most mono- and polyunsaturated LPCs and LPEs were present in lower concentrations in H progression diet group, relative to C or E. This is consistent with results in mouse serum<sup>[41]</sup> and liver<sup>[42]</sup> but in contrast to those in pig colons.<sup>[43]</sup> The discrepancies between LPC/LPE fatty acyl chain saturation in previous reports may be due to tissue-specific differences, and represents an understudied area in diet associations with fatty acyl tail saturation.

#### 4.2. Metabolites Associated with ACF

Increased concentrations of LPCs, LPEs, and phosphatidylethanolamines (PEs) were observed in animals that developed ACF, as compared to those without ACF. Increased levels of LPCs and LPEs have also been reported in women with stage 1 right-sided CRC, relative to adjacent normal tissue.<sup>[44]</sup> LPCs may participate with diacylglycerols to sustain protein kinase C (PKC) signaling,<sup>[45]</sup> which promotes cell proliferation and carcinogenesis<sup>[46]</sup> and may contribute to ACF formation.

**Table 4.** Identities of metabolites that met fold-change and *p*-value cutoffs in ACF comparisons (FDR-adjusted *p*-value  $\leq 0.05$  and top 20 positive and negative estimate value for ACF term in Equation (2), see Figure 3).

<i>m/z</i> <sup>a)</sup>	RT	Precursor ion	Mode	Class	ID	ID level
<b>Increased in ACF presence</b>						
604.3498	3.76	[M+C <sub>2</sub> H <sub>3</sub> O <sub>2</sub> ] <sup>-</sup>	Neg	Lysophosphatidylcholine	LPC(20:3)	2
538.3510	3.79	[M-H+H <sub>2</sub> O] <sup>-</sup>	Neg	Lysophosphatidylcholine	LPC(16:1)	3
468.3121	3.85	[M+H] <sup>+</sup>	Pos	Lysophosphatidylethanolamine	LPE(17:0)	2
768.5431	2.25	[M+Cl] <sup>-</sup>	Neg	Phosphatidylcholine	PC(16:0/16:0)	1
718.5771	2.71	[M+H] <sup>+</sup>	Pos	Phosphatidylcholine	PE(16:0/18:1)	1
706.5437	2.84	[M+H] <sup>+</sup>	Pos	Phosphatidylcholine	PC(14:0/16:0)	2
720.5437	2.81	[M+H] <sup>+</sup>	Pos	Ether phosphatidylcholine	PC(O-32:0)	3
692.5505	2.80	[M+H] <sup>+</sup>	Pos	Ether phosphatidylcholine	PC(O-30:3)	3
688.4994	3.28	[M-H] <sup>-</sup>	Neg	Phosphatidylethanolamine	PE(16:0/16:1)	2
674.5156	3.08	[M+H] <sup>+</sup>	Pos	Phosphatidylethanolamine plasmalogen	PE(P-16:0/16:1)	3
807.5007	3.66	[M-H] <sup>-</sup>	Neg	Phosphatidylinositol	PI(16:0/16:1)	2
<b>Increased in ACF absence</b>						
124.0073	5.41	[M-H] <sup>-</sup>	Neg	Amino acid	Taurine	1
419.2559	2.31	[M-H] <sup>-</sup>	Neg	Cyclophosphatidic acid	CPA(18:0)	2
466.3261	4.07	[M-H] <sup>-</sup>	Neg	Ether phosphatidylethanolamine	PE(O-18:0)	2
282.0843	4.45	[M-H] <sup>-</sup>	Neg	Purine	guanosine	1
167.0211	5.18	[M-H] <sup>-</sup>	Neg	Purine	uric acid	1
137.0462	3.60	[M+H] <sup>+</sup>	Pos	Purine	hypoxanthine	1
267.0734	3.72	[M-H] <sup>-</sup>	Neg	Purine	inosine	1

<sup>a)</sup> Unknown metabolites (level 4 ID) in Table S4, Supporting Information.

Increased concentrations of PEs in mice that developed ACF are also consistent with studies of human CRC tissue, in which phosphoethanolamine (the headgroup of PEs) was increased relative to healthy adjacent tissue<sup>[47]</sup> or healthy adjacent mucosa.<sup>[48,49]</sup> This likely reflects increased cell proliferation in early CRC.

Purines were also decreased in mice that developed AOM-induced ACF, relative to mice that did not develop ACF. Likewise, rats receiving AOM alone had decreased concentrations of hypoxanthine relative to those receiving AOM + resveratrol (to prevent ACF formation), or a vehicle control.<sup>[50]</sup> In contrast, increased levels of purines have been reported in most human studies of CRC tissue, relative to normal adjacent tissue.<sup>[51–54]</sup> Limited purine availability may reflect more rapid cellular turnover and could contribute to increased DNA mismatch repair, resulting in imbalanced nucleotide pools in ACF-carrying mice. Indeed, viral or cellular activators of aberrant cell proliferation applied to keratinocytes *in vitro* also resulted in decreased concentrations of nucleotides, despite increased cell proliferation.<sup>[55]</sup> The infected cells also exhibited increased loss of heterozygosity at fragile sites over time, a common effect of chromosomal instability found in  $\approx 70\%$  of all sporadic CRC.<sup>[56]</sup> Exogenous application of nucleotides spared the cells from DNA damage induced by replication stress. The authors hypothesized that early cancer development involves increased cell proliferation, signaled by oncogene expression, in the absence of a sufficient nucleotide pool, leading to genomic instability.<sup>[55]</sup> This hypothesis is consistent with the observations reported herein of decreased purines in the mice that developed ACF. Expression of these genes and metabo-

lites over the course of cancer development requires further study, as decreased purines may be associated with early cancer development.

Taurine was decreased in mice that developed ACF, compared to mice that did not develop ACF. In contrast, exogenous taurine decreased ACF formation in a dose-dependent manner<sup>[57]</sup> and decreased tumor formation in mice.<sup>[58]</sup> Taurine concentrations are also consistently higher in CRC tissue relative to normal colon tissue.<sup>[53,59–62]</sup> These discrepancies suggest different roles for taurine as colorectal carcinogenesis progresses.

#### 4.3. Lack of ACF:Diet Interaction

No significant diet:ACF interactions were observed. While some metabolite classes met cutoffs for both diet and ACF comparisons, the lack of interaction likely reflects the lack of difference in ACF presence across diet groups (*p*-values = 0.1–0.7).

One major strength of this study was the ability to directly compare the metabolomic profiles of colons in mice fed H, E, or C diets in the same sample population. Additionally, the transition from initiation to progression diets after azoxymethane treatment represents diet changes commonly observed in humans throughout their lifespan. The use of ACF as a marker of early CRC development enables hypothesis generation about metabolite-mediated pathways associated with early phases of CRC progression. However, the lack of overt tumor formation, a limitation previously reported for this strain of animals, restricts translation of these results to CRC. The substantial number

of metabolites identified in this untargeted study allowed for proposal of many potential pathways in early CRC. However, the small masses of colon tissue available, and the low intensity of metabolite signals which overlapped with those of impurities arising from the extraction process, limited the ability to detect significant metabolites by <sup>1</sup>H-NMR. Additionally, the signal available for MS/MS fragmentation of some metabolites for identification, which limits some of this interpretation. Limited signal also likely limited the ability to detect metabolites previously identified as different in previous H versus C and E versus C studies.<sup>[18,19]</sup> Additionally, the monophasic extraction captured lipid species not commonly captured by HILIC-LC-MS. The lack of a vehicle control also makes it difficult to ascribe differences in metabolite formation to ACF development, rather than AOM administration. Finally, study of these metabolites in more easily accessible biospecimens—such as plasma, urine, or stool—is an important next step in identifying putative biomarkers of ACF presence.

## 5. Conclusions

Consumption of progression H, E, or C diets (but not initiation diets) were significantly associated with acylcarnitine and phospholipid metabolite abundances in mouse colon extracts. Phospholipids, purines, and taurine were also associated with ACF-present versus absent mice after AOM administration. No interaction of diet:ACF formation was observed. Results suggest differences in metabolite abundances that may be influenced by disease stage. Further study of the relative levels and pathways of these metabolites over the course of CRC is warranted.

## Supporting Information

Supporting Information is available from the Wiley Online Library or from the author.

## Acknowledgements

The authors would like to thank Kevin Ying and Dr. Jalal Siddiqi for their assistance in sample weighing, Dr. Matthew Bernier for assistance with LC-MS instrumentation, Dr. Joseph McElroy for assistance with statistical models, and John Braisted for his insight into RaMP for pathway analyses. Part of the sample analysis was supported by NIH Award Number Grant P30 CA016058, OSU, and OSUCCC. This work was also supported in part by the Intramural Research Program of the National Center for Advancing Translational Sciences, National Institutes of Health (1Z1CTR000410-02).

## Conflict of Interest

The authors declare no conflict of interest.

## Author Contributions

H.A.C. and C.A.R. contributed equally to this work. E.A.M., E.H., and R.E.K. ideated the project and provided funding; S.O.M. and M.B. conducted the parent animal study and provided the samples; H.C., E.H., and R.E.K. conducted sample analyses and metabolite annotation; C.R., H.C., K.S., J.M., and E.A.M. performed data analysis; H.C., C.R., K.S. wrote original draft; all authors edited and approved the final draft; E.A.M. and R.E.K. were responsible for the contents of the final manuscript.

## Data Availability Statement

The data that support the findings of this study are openly available at Figshare, in the DOIs listed in Table 1 of the manuscript.

## Keywords

colorectal cancer, dietary energy intake, liquid chromatography-mass spectrometry, regression analysis, untargeted metabolomics

Received: March 22, 2022

Revised: July 12, 2022

Published online: September 30, 2022

- [1] H. Sung, J. Ferlay, R. L. Siegel, M. Laversanne, I. Soerjomataram, A. Jemal, F. Bray, *Ca-Cancer J. Clin.* **2021**, *71*, 209.
- [2] R. L. Siegel, K. D. Miller, S. A. Fedewa, D. J. Ahnen, R. G. S. Meester, A. Barzi, A. Jemal, *Ca-Cancer J. Clin.* **2017**, *67*, 177.
- [3] E. H. Schreuders, A. Ruco, L. Rabeneck, R. E. Schoen, J. J. Y. Sung, G. P. Young, E. J. Kuipers, *Gut* **2015**, *64*, 1637.
- [4] S. J. Alrawi, M. Schiff, R. E. Carroll, M. Dayton, J. F. Gibbs, M. Kulavlat, D. Tan, K. Berman, D. L. Stoler, G. R. Anderson, *Anticancer Res.* **2006**, *26*, 107.
- [5] G. Binefa, F. Rodríguez-Moranta, À. Teule, M. Medina-Hayas, *World J. Gastroenterol.* **2014**, *20*, 6786.
- [6] E. A. Platz, W. C. Willett, G. A. Colditz, E. B. Rimm, D. Spiegelman, E. Giovannucci, *Cancer Causes Control* **2000**, *11*, 579.
- [7] B. Magalhães, B. Peleteiro, N. Lunet, *Eur. J. Cancer Prev.* **2012**, *21*, 15.
- [8] M. L. Slattery, K. M. Boucher, B. J. Caan, J. D. Potter, K.-N. Ma, *Am. J. Epidemiol.* **1998**, *148*, 4.
- [9] M. L. Slattery, J. D. Potter, K. N. Ma, B. J. Caan, M. Leppert, W. Samowitz, *Cancer Causes Control* **2000**, *11*, 1.
- [10] A. M. O'Neill, C. M. Burrington, E. A. Gillaspie, D. T. Lynch, M. J. Horsman, M. W. Greene, *Nutr. Res.* **2016**, *36*, 1325.
- [11] H. Zeng, S. L. Ishaq, Z. Liu, M. R. Bukowski, *J. Nutr. Biochem.* **2018**, *54*, 18.
- [12] S. D. Day, R. T. Enos, J. L. McClellan, J. L. Steiner, K. T. Velázquez, E. A. Murphy, *Cytokine* **2013**, *64*, 454.
- [13] A. E. Harvey, L. M. Lashinger, G. Otto, N. P. Nunez, S. D. Hursting, *Mol. Carcinog.* **2013**, *52*, 997.
- [14] S. E. Olivo-Marston, S. D. Hursting, S. N. Perkins, A. Schetter, M. Khan, C. Croce, C. C. Harris, J. Lavigne, *PLoS One* **2014**, *9*, <https://doi.org/10.1038/srep19083>
- [15] V. Mai, L. H. Colbert, D. Berrigan, S. N. Perkins, R. Pfeiffer, J. A. Lavigne, E. Lanza, D. C. Haines, A. Schatzkin, S. D. Hursting, *Cancer Res.* **2003**, *63*, 1752.
- [16] E. Svensson, B. Møller, S. Tretli, L. Barlow, G. Engholm, E. Pukkala, M. Rahu, L. Tryggvadóttir, F. Langmark, T. Grotmol, *Cancer Causes Control* **2005**, *16*, 215.
- [17] L. A. E. Hughes, P. A. van den Brandt, A. P. de Bruïne, K. A. D. Wouters, S. Hulsmans, A. Spiertz, R. A. Goldbohm, A. F. P. M. de Goeij, J. G. Herman, M. P. Weijenberg, M. van Engeland, *PLoS One* **2009**, *4*, e7951.
- [18] D. Dermadi, S. Valo, S. Ollila, R. Soliymani, N. Sipari, M. Pussila, L. Sarantaus, J. Linden, M. Baumann, M. Nyström, *Cancer Res.* **2017**, *77*, 3352.
- [19] C. L. Green, Q. A. Soltow, S. E. Mitchell, D. Deros, Y. Wang, L. Chen, J. D. J. Han, D. E. L. Promislow, D. Lusseau, A. Douglas, D. P. Jones, J. R. Speakman, *J. Gerontol. - Ser. A Biol. Sci. Med. Sci.* **2019**, *74*, 16.
- [20] J. Xu, J. D. Galley, M. T. Bailey, J. M. Thomas-Ahner, S. K. Clinton, S. E. Olivo-Marston, *Sci. Rep.* **2016**, *6*, 19083.

- [21] Z. Z. Tang, G. Chen, Q. Hong, S. Huang, H. M. Smith, R. D. Shah, M. Scholz, J. F. Ferguson, *Front. Genet.* **2019**, *10*, <https://doi.org/10.3389/fgene.2019.00454>.
- [22] G. A. Nagana Gowda, D. Djukovic, L. F. Bettcher, H. Gu, D. Raftery, *Anal. Chem.* **2018**, *90*, 2001.
- [23] G. James, D. Witten, T. Hastie, R. Tibshirani, "ISLR: Data for an Introduction to Statistical Learning with Applications in R" **2017**, <https://cran.r-project.org/web/packages/ISLR/ISLR.pdf>.
- [24] J. Pinheiro, D. Bates, S. DebRoy, D. Sarkar, R. C. Team, "nlme: Linear and Nonlinear Mixed Effects Models," n.d., <https://cran.r-project.org/package=nlme>.
- [25] L. W. Sumner, A. Amberg, D. Barrett, M. H. Beale, R. Beger, C. A. Daykin, T. W. M. Fan, O. Fiehn, R. Goodacre, J. L. Griffin, T. Hankemeier, N. Hardy, J. Harnly, R. Higashi, J. Kopka, A. N. Lane, J. C. Lindon, P. Marriott, A. W. Nicholls, M. D. Reily, J. J. Thaden, M. R. Viant, *Metabolomics* **2007**, *3*, 211.
- [26] D. S. Wishart, Y. D. Feunang, A. Marcu, A. C. Guo, K. Liang, R. Vázquez-Fresno, T. Sajed, D. Johnson, C. Li, N. Karu, Z. Sayeeda, E. Lo, N. Assempour, M. Berjanskii, S. Singhal, D. Arndt, Y. Liang, H. Badran, J. Grant, A. Serra-Cayuela, Y. Liu, R. Mandal, V. Neveu, A. Pon, C. Knox, M. Wilson, C. Manach, A. Scalbert, *Nucleic Acids Res.* **2018**, *46*, D608.
- [27] M. Sud, E. Fahy, D. Cotter, A. Brown, E. Dennis, C. Glass, R. Murphy, C. Raetz, D. Russell, S. Subramaniam, *Nucleic Acids Res.* **2006**, *35*, D527.
- [28] J. Braisted, A. Patt, C. Tindall, T. Eicher, T. Sheils, J. Neyra, K. Spencer, E. A. Mathé, *bioRxiv* **2022**, <https://doi.org/10.1101/2022.01.19.476987>
- [29] B. P. Sampey, A. J. Freermerman, J. Zhang, P. F. Kuan, J. A. Galanko, T. M. O'Connell, O. R. Ilkayeva, M. J. Muehlbauer, R. D. Stevens, C. B. Newgard, H. A. Brauer, M. A. Troester, L. Makowski, *PLoS One* **2012**, *7*, <https://doi.org/10.1371/journal.pone.0038812>
- [30] S. Goethals, C. Rombouts, L. Y. Hemeryck, L. Van Meulebroek, T. Van Hecke, E. Vossen, J. Van Camp, S. De Smet, L. Vanhaecke, *Mol. Nutr. Food Res.* **2020**, *64*, <https://doi.org/10.1002/mnfr.202000070>
- [31] P. D. Chandler, R. Balasubramanian, N. Paynter, F. Giulianini, T. Fung, L. F. Tinker, L. Snetselaar, S. Liu, C. Eaton, D. K. Tobias, F. K. Tabung, J. A. E. Manson, E. L. Giovannucci, C. Clish, K. M. Rexrode, *Am. J. Clin. Nutr.* **2020**, *112*, 268.
- [32] I. R. Schlaepfer, M. Joshi, *Endocrinol. (United States)* **2020**, *161*, <https://doi.org/10.1210/endo/bqz046>
- [33] C. S. McCoin, T. A. Knotts, S. H. Adams, *Nat. Rev. Endocrinol.* **2015**, *11*, 617.
- [34] T. Minami, H. Tojo, Y. Shinomura, Y. Matsuzawa, M. Okamoto, *Gut* **1994**, *35*, 1593.
- [35] D. Wendum, M. Svrcek, V. Rigau, P. Y. Boëlle, N. Sebbagh, R. Parc, J. Masliah, G. Trugnan, J. F. Fléjou, *Mod. Pathol.* **2003**, *16*, 130.
- [36] W. Stremmel, R. Ehehalt, S. Staffer, S. Stoffels, A. Mohr, M. Karner, A. Braun, *Dig. Dis.* **2013**, *30*, 85.
- [37] W. Stremmel, H. Vural, O. Evliyaoglu, R. Weiskirchen, *Dig. Dis.* **2021**, *39*, 508.
- [38] B. Wang, P. Tontonoz, *Annu. Rev. Physiol.* **2019**, *81*, 165.
- [39] M. Bagherniya, A. E. Butler, G. E. Barreto, A. Sahebkar, *Ageing Res. Rev.* **2018**, *47*, 183.
- [40] L. M. Z. Lafave, P. Kumarathasan, R. P. Bird, *Lipids* **1994**, *29*, 693.
- [41] J. H. Shin, M. H. Nam, H. Lee, J. S. Lee, H. Kim, M. J. Chung, J. G. Seo, *Eur. J. Nutr.* **2018**, *57*, 2081.
- [42] M. Nam, M. S. Choi, J. Y. Choi, N. Kim, M. S. Kim, S. Jung, J. Kim, D. H. Ryu, G. S. Hwang, *J. Nutr. Biochem.* **2018**, *51*, <https://doi.org/10.1002/mnfr.201900811>
- [43] K. Hanhineva, T. Barri, M. Kolehmainen, J. Pekkinen, J. Pihlajamäki, A. Vesterbacka, G. Solano-Aguilar, H. Mykkänen, L. O. Dragsted, J. F. Urban, K. Poutanen, *J. Proteome Res.* **2013**, *12*, 3980.
- [44] Y. Cai, N. J. W. Rattray, Q. Zhang, V. Mironova, A. Santos-Neto, K. S. Hsu, Z. Rattray, J. R. Cross, Y. Zhang, P. B. Paty, S. A. Khan, C. H. Johnson, *Sci. Rep.* **2020**, *10*, <https://doi.org/10.1038/s41598-020-61851-0>
- [45] Y. Nishizuka, *FASEB J.* **1995**, *9*, 484.
- [46] J.-H. Kang, *New J. Sci.* **2014**, *2014*, <https://doi.org/10.1155/2014/231418>
- [47] M. Mal, P. K. Koh, P. Y. Cheah, E. C. Y. Chan, *Anal. Bioanal. Chem.* **2012**, *403*, 483.
- [48] A. Mika, A. Pakiet, A. Czumaj, Z. Kaczynski, I. Liakh, J. Kobiela, A. Perdyan, K. Adrych, W. Makarewicz, T. Sledzinski, *J. Clin. Med.* **2020**, *9*, 1095.
- [49] T. E. Merchant, J. N. Kasimos, P. W. de Graaf, B. D. Minsky, L. W. Gierke, T. Glonek, *Int. J. Colorectal Dis.* **1991**, *6*, 121.
- [50] W. Liao, H. Wei, X. Wang, Y. Qiu, X. Gou, X. Zhang, M. Zhou, J. Wu, T. Wu, F. Kou, Y. Zhang, Z. Bian, G. Xie, W. Jia, *J. Proteome Res.* **2012**, *11*, 3436.
- [51] Y. Tian, T. Xu, J. Huang, L. Zhang, S. Xu, B. Xiong, Y. Wang, H. Tang, *Sci. Rep.* **2016**, *6*, <https://doi.org/10.1038/srep20790>
- [52] C. Denkert, J. Budczies, W. Weichert, G. Wohlgemuth, M. Scholz, T. Kind, S. Niesporek, A. Noske, A. Buckendahl, M. Dietel, O. Fiehn, *Mol. Cancer* **2008**, *7*, 72.
- [53] E. Chun Yong Chan, P. Koon Koh, M. Mal, P. Yean Cheah, K. Weng Eu, A. Backshall, R. Cavill, J. K. Nicholson, H. C. Keun, *J. Proteome Res.* **2009**, *8*, 352.
- [54] D. G. Brown, S. Rao, T. L. Weir, M. Bazan, R. J. Brown, E. P. Ryan, *Cancer Metab.* **2016**, *4*, <https://doi.org/10.1186/s40170-016-0151-y>
- [55] A. C. Bester, M. Roniger, Y. S. Oren, M. M. Im, D. Sarni, M. Chaoat, A. Bensimon, G. Zamir, D. S. Shewach, B. Kerem, *Cell* **2011**, *145*, 435.
- [56] E. J. Poulin, J. Shen, J. J. Gierut, K. M. Haigis, *Pathol. Epidemiol. Cancer* **2017**, *1*, 409.
- [57] M. J. Wargovich, A. Jimenez, K. McKee, V. E. Steele, M. Velasco, J. Woods, R. Price, K. Gray, G. J. Kelloff, *Carcinogenesis* **2000**, *21*, 1149.
- [58] G. Wang, G. Wang, N. Ma, N. Ma, F. He, S. Kawanishi, H. Kobayashi, S. Oikawa, M. Murata, *Oxid. Med. Cell. Longev.* **2020**, *2020*, 1.
- [59] A. Moreno, M. Rey, J. M. Montane, J. Alonso, C. Arús, *NMR Biomed.* **1993**, *6*, 111.
- [60] A. Moreno, C. Arús, *NMR Biomed.* **1996**, *9*, 33.
- [61] W. Chen, X. Zhou, D. Huang, F. Chen, X. Du, *Chinese J. Chem.* **2011**, *29*, 2511.
- [62] M. Piotto, F. M. Moussallieh, B. Dillmann, A. Imperiale, A. Neuville, C. Brigand, J. P. Bellocq, K. Elbayed, I. J. Namer, *Metabolomics* **2009**, *5*, 292.